

## Supporting Information

### On the structure of the $N_x$ phase of symmetric dimers: inferences from NMR

Anke Hoffmann<sup>1</sup>, Alexandros G. Vanakaras<sup>2</sup>, Alexandra Kohlmeier<sup>3</sup>,

Georg H. Mehl<sup>3</sup>, Demetri J. Photinos<sup>2</sup>

<sup>1</sup> Department of Inorganic and Analytical Chemistry, University of Freiburg, 79104  
Freiburg, Germany

<sup>2</sup> Department of Materials Science, University of Patras, Patras26504, Greece

<sup>3</sup> Department of Chemistry, University of Hull, Hull, HU6 7RX, UK

*This supporting information file contains details on the NMR measurement and analysis of the measured spectra, a discussion of the influence of rotational viscosity on the NMR spectra and a comparison with the spectra that would be obtained for a hypothetical heliconical configuration of the director according to the twist-bend proposal for the  $N_x$  phase. Preparation of the target material. The DSC of the studied compound is also included.*

#### 1. Details of NMR measurements

**1.1 Experiments.** All spectra were measured on a BrukerAvance 500 NMR spectrometer ( $B_0=11.7\text{ T}$ ,  $\nu_{2H}=76.8\text{ Hz}$ ). Solid echo experiments were performed with  $90^\circ$  pulse length of  $4\ \mu\text{s}$  and a pulse spacing of  $43\ \mu\text{s}$ . For the rotation of the sample a homebuilt probehead with a servomotor was used, triggered from the NMR console (Figure S1a). The sample can be rotated around a fixed axis perpendicular to the magnetic field. Samples were prepared by filling the substance into a 2 cm long glass tube with 4 mm diameter and sealed with a teflon/silicon plug (punched out from a

septum). This tube was then fixed in the middle of a 5mm glass tube making use of teflon band (Figure S1b). The flipping experiments were performed by flipping the sample by  $90^\circ$  around an axis perpendicular to the static magnetic field, data acquisition, and then flipping the sample back to the initial position for the recycle delay (1s). The acquisition starts (earliest) 200 ms after triggering the sample flip, which is the time at which the sample has definitely reached the new orientation. This has been tested extensively with standard samples to get the proper timing and to verify the precision of the angular setting and test the fixation of the sample. Also, this probe has been in use for several years and has been proven to give reliable results for several low molecular weight as well as polymeric liquid crystals.

The spinning experiment spectra shown in Fig 2c were recorded with 100 *rpm* spinning rate about an axis perpendicular to the static magnetic field. Spectra recorded with 6, 60 and 200 *rpm* showed no significant differences at the given temperature. Cooling and heating sequences were run with temperature steps of 1K. After each step the sample was equilibrated for 10 minutes before the start of the acquisition. For the experiments under  $90^\circ$  flipping and under continuous spinning the sample was heated to the isotropic phase and then slowly cooled to the desired temperature. The splittings obtained from different cooling runs agree within an error of less than 1%.

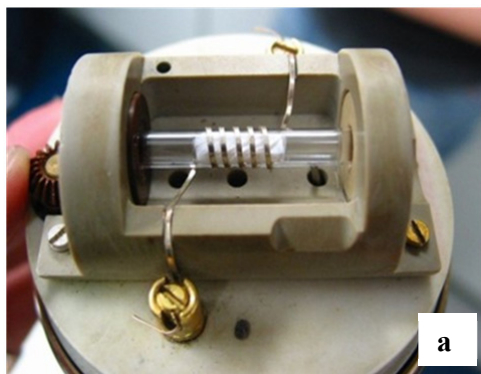
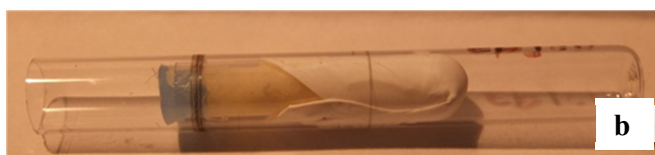


**Figure S1** a.) Probe with a mounted sample tube (not CB-C9-CB). Cog-wheel for rotation can be seen on the left.

b.) Sample tube containing CB-C9-CB.



## 1.2 Analysis of measured spectra.

### *(a) Aligned sample spectra.*

The doubling of each of the quadrupolar peaks of the  $\alpha$ -CD<sub>2</sub> sites in the N<sub>X</sub> phase produces two sub-peaks of different heights and widths. Specifically, the height of the outer sub-peak is appreciably lower but its width is larger than that of the inner sub-peak. The integrated intensity, as it comes out from the direct manual integration in the NMR software is about 10% smaller for the outer peaks. However, this neglects the fact that a part of the outer peaks (the asymmetric ‘foot’ to the middle) lies underneath the inner peaks. When this is taken into account the relative intensities are readily shifted to equality, within the experimental resolution. Furthermore, the simulation of the spectra recorded under continuous rotation, discussed in the next section, is based on summing the two sub-peaks with equal integrated intensities and this yields the essentially exact agreement with the measured spectral distribution of intensity.

### *(b) Spinning sample spectra.*

The experimental spectra obtained under continuous spinning of the sample about an axis perpendicular to the magnetic field were simulated by a powder sum for cylindrical distribution of the nematic directors (i.e. without a scaling factor  $\sin(\beta)$  as for spherical distribution), namely

$$I(t) = \sum_{i=1}^N \cos(2\pi\delta_Q(3\cos^2(\beta_i) - 1)t)$$

Where  $\delta_Q$  is the anisotropy of the (time averaged) quadrupolar coupling tensor; the asymmetry of the tensor is neglected. A set of 200 polar angles  $\beta$ , equally distributed in the range of 0 to  $\pi$ , was used (i.e.  $N=200$ ; a simulation with  $N=400$  showed no significant differences). The spectrum shown in figure 2(c) was simulated as the sum of two cylindrical powder patterns with anisotropies  $\delta_Q$  of 28 kHz and 20.2 kHz – the values of the quadrupolar splitting obtained from the temperature run (Fig 1c). The patterns were added without additional weighting factors (i.e. the two patterns have the same integrated intensity) and scaled to the height of the inner peaks of the experimental spectrum.

### *(c) Simulation of the aligned and 90° –flipped spectra in the N<sub>X</sub> phase.*

In figure S2 we present the experimental NMR spectra of the aligned (red) and of the flipped by 90° with respect to magnetic field samples, (see also fig Fig 2(a) of the

paper). Best fitting curves are also shown for both sets of measured spectra. The line shapes,  $L_{0(90)}(\nu)$ , of these spectra are fitted assuming a superposition of two Lorentzians  $\Lambda(\nu; \delta\nu, w) = w / (\pi(w^2 + (\nu - \delta\nu)^2))$  of the *same integrated intensity*:

$$L_{\theta_{H,n}}(\nu) = \sum_{r=\pm 1} \Lambda\left(\nu; r \frac{\delta\nu_Q(\theta_{H,n})}{2}, w_0(\theta_{H,n})\right) + \Lambda\left(\nu; r \frac{\delta\nu'_Q(\theta_{H,n})}{2}, w'_0(\theta_{H,n})\right) \quad (\text{S.1})$$

Here  $\theta_{H,n} = 0$  or  $90$  denotes the angle between the magnetic field and the director for the aligned and the  $90^\circ$ -flipped samples, respectively.

**Table I.** Best-fit parameters for the simulated spectra with eq (S.1).

$\theta_{H,n}$	$\delta\nu_Q(\theta_{H,n}) / 2$	$w_0(\theta_{H,n})$	$\delta\nu'_Q(\theta_{H,n}) / 2$	$w'_0(\theta_{H,n})$
$0^\circ$	26.958	0.734	21.134	0.380
$90^\circ$	13.545	0.374	10.486	0.260

We note here that for both peaks we have,  $\delta\nu(90) = \delta\nu(0) / 2$  and  $\delta\nu'(90) = \delta\nu'(0) / 2$ , indicating uniaxial ordering in the sample, to within experimental resolution.

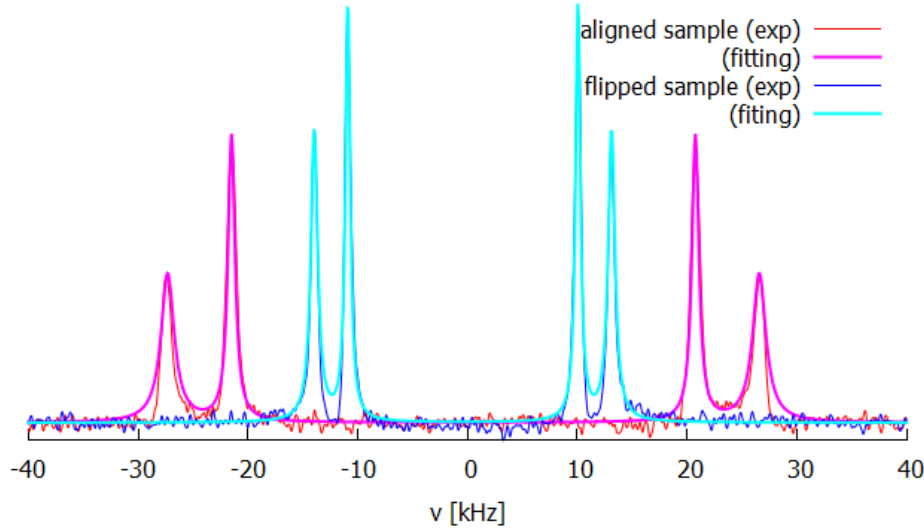


**Figure S2:**  $^2\text{HNMR}$  spectra of the aligned sample (red) and after a flip by  $90^\circ$  with respect to the magnetic field (blue) in the  $N_x$  phase at  $90^\circ\text{C}$ . The thick lines (magenta for the aligned sample and cyan for the  $90^\circ$ -flipped) are simulated spectra assuming Lorentzian line-shapes according to eq(S.1), with the best-fit parameter values listed in Table I.

## 2. The effects of viscosity on the $90^\circ$ -rotated and spinning sample spectra.

At 80°C, spectra recorded under continuous spinning (Figure 2(c)) showed no significant difference when recorded with spinning rates of 6 *rpm*, 60*rpm*, 100 *rpm* and 200 *rpm*. This independence on the spinning rate indicates that a uniform cylindrical distribution of the nematic director is generated by the spinning of the sample and that such distribution is not influenced by hydrodynamic effects, as these would show a dependence on the spinning-rate. Furthermore, the spectra had not relaxed back to equilibrium two hours after the rotation was stopped. Such slow relaxation rates, together with the absence of significant hydrodynamic effects on spinning, are direct implications of the high viscosity of the N<sub>X</sub> phase.

The orientational relaxation times show a relatively rapid variation with temperature within the N<sub>X</sub> phase and a dramatic drop on entering the N phase. Thus, the spectra shown in Figure 2(b), recorded at the temperature of 90°C, are not fully relaxed 10s after the 90° flip. A respective spectrum recorded at 100°C is only partially relaxed after 4s. At 104 °C, the spectra recorded under continuous spinning look different for 1*rpm*, 6*rpm*, 60*rpm*, indicating the onset of appreciable hydrodynamic effects on the director distribution. Lastly, at 106°C, near the onset of the N phase range, the spectra before and after the 90° flip are identical, indicating that the orientation fully relaxes within less than 200 *ms*. Spectra recorded under continuous spinning still show a single splitting for rotation up to 2000 *rpm*; only for rotations of 4000 *rpm* and 5000 *rpm* the spectra get broad. Accordingly, the orientational relaxation time ( $\sim 10^{-3}$ sec) at this temperature is four orders of magnitude faster than the respective time ( $\sim 10$  sec) at the temperature of 90°C in the N<sub>X</sub> phase.

### 3. Spectral line-shape for a hypothetical heliconical configuration with the magnetic field perpendicular to the helix axis

As detailed in the main text the measured 90°-rotated and spinning sample NMR spectra indicate rather directly that the entire sample exhibits a single, uniform, director. Here we present the calculation of the NMR spectrum of a sample assuming that the  $N_X$  phase is a twist-bent nematic presenting a heliconical distribution of the director field. The calculated spectra are then contrasted with the measured spectra. As indicated in the main text, the splitting associated with an  $\alpha$ -C-D bond, is given by the ensemble average:

$$\delta\nu_Q = \nu_Q \left\langle \frac{3}{2} (\hat{H} \cdot \hat{e}_{\alpha-CD})^2 - \frac{1}{2} \right\rangle \quad (\text{S.2})$$

Where  $\hat{H}$  denotes the direction of the magnetic field,  $\hat{e}_{\alpha-CD}$  the direction of the C-D bond and  $\nu_Q = -3q_{CD} / 2$ . In a uniaxial nematic phase, with the director denoted by  $\hat{n}$ , the splitting can be expressed in terms of the ‘‘bond order parameter’’

$$S_{\alpha-CD}^{(n)} \equiv \left\langle \frac{3}{2} (\hat{n} \cdot \hat{e}_{\alpha-CD})^2 - \frac{1}{2} \right\rangle \quad (\text{S.3})$$

and the orientation of the director relative to the magnetic field as follows:

$$\delta\nu_Q = \nu_Q S_{\alpha-CD}^{(n)} \left( \frac{3}{2} (\hat{H} \cdot \hat{n})^2 - \frac{1}{2} \right) \quad (\text{S.4})$$

With the help of equations (S.2)-(S.4) we can calculate the spectral line-shape for a hypothetical heliconical configuration with the magnetic field perpendicular to the helix axis, obtained by 90-flip of the aligned sample about an axis perpendicular to the magnetic field: In a macroscopic frame where the  $Z$  axis is identified with the helix axis and the direction of the magnetic field (perpendicular to the helix axis) is identified with the  $Y$  axis, the assumed heliconical distribution of the director,  $\hat{n} = (\sin \theta_0 \cos kZ, \sin \theta_0 \sin kZ, \cos \theta_0)$ , would imply the following distribution of the directional term in the rhs of eq (S.4) over the angle  $\varphi = kZ$ ,

$$\frac{3}{2} (\hat{H} \cdot \hat{n})^2 - \frac{1}{2} = \frac{3}{2} (\sin \theta_0 \sin \varphi)^2 - \frac{1}{2} \quad (\text{S.5})$$

In this case we have, according to eq(S.4) a  $\varphi$ -distribution of splittings,

$$\delta\nu_Q(\theta_0, \varphi) = \frac{\nu_Q S_{\alpha-CD}^{(n)}}{2} (3(\sin \theta_0 \sin \varphi)^2 - 1) = \frac{\delta\nu_Q(0)}{2} (3(\sin \theta_0 \sin \varphi)^2 - 1) \quad (\text{S.6})$$

where  $\delta\nu_{\rho}(0) = \nu_{\rho}S_{\alpha-CD}^{(n)}$  is the ‘‘aligned sample splitting’’, obtained when the director is parallel to the magnetic field.

The NMR spectrum of a heliconalnematic with ‘‘tilt’’ angle  $\theta_0$  will be simply the uniform superposition of line-shapes of the form  $\Lambda\left(\nu; \pm\delta\nu_{\rho}(\theta_0, \varphi), w(\theta_0, \varphi)\right)$  for all possible angles  $0 < \varphi < 2\pi$ ,

$$f_{90\text{-flip}}(\nu) = \frac{1}{2\pi} \int_0^{2\pi} d\varphi \sum_{r=\pm 1} \left( \Lambda\left(\nu; r \frac{\delta\nu_{\rho}(0)}{4} \left(3(\sin\theta_0 \sin\varphi)^2 - 1\right), w(\varphi)\right) + \Lambda\left(\nu; r \frac{\delta\nu'_{\rho}(0)}{4} \left(3(\sin\theta_0 \sin\varphi)^2 - 1\right), w'(\varphi)\right) \right) \quad (\text{S.7})$$

In eq (S.7) the parameters  $\delta\nu_{\rho}(0)$  and  $\delta\nu'_{\rho}(0)$  are the experimental ‘‘aligned sample splitting’’. For the angular dependence of the line-widths we have used the standard form (see refs. <sup>1</sup>)  $w(\hat{H} \cdot \hat{n}) = w(0) + 2(w(0) - w(90))( |P_2(\hat{H} \cdot \hat{n})| - 1)$  and similarly for  $w'(\hat{H} \cdot \hat{n})$ , with the values of  $w(0), w(90), w'(0), w'(90)$  taken from Table I. The calculated NMR spectra using eq (S.7) for various values of the ‘‘tilt’’ angle  $\theta_0$  are presented in figure S3. These results demonstrate clearly that when  $\theta_0 = 0$  (no heliconal structure) the calculated spectrum coincides practically with the experimental spectrum while a deviation becomes apparent by simple visual inspection already from  $\theta_0 = 10^\circ$ . The deviation from the measured spectral patterns become rapidly more pronounced, leading to a totally different spectrum, for larger values of  $\theta_0$ .

---

<sup>1</sup>P. J. Collings, D. J. Photinos, P. J. Bos, P. Ukleja, and J. W. Doane, Phys. Rev. Lett. **42**, 996 (1979).

D. J. Photinos, P. J. Bos, J. W. Doane, and M. E. Neubert, Phys. Rev. A **20**, 2203 (1979).

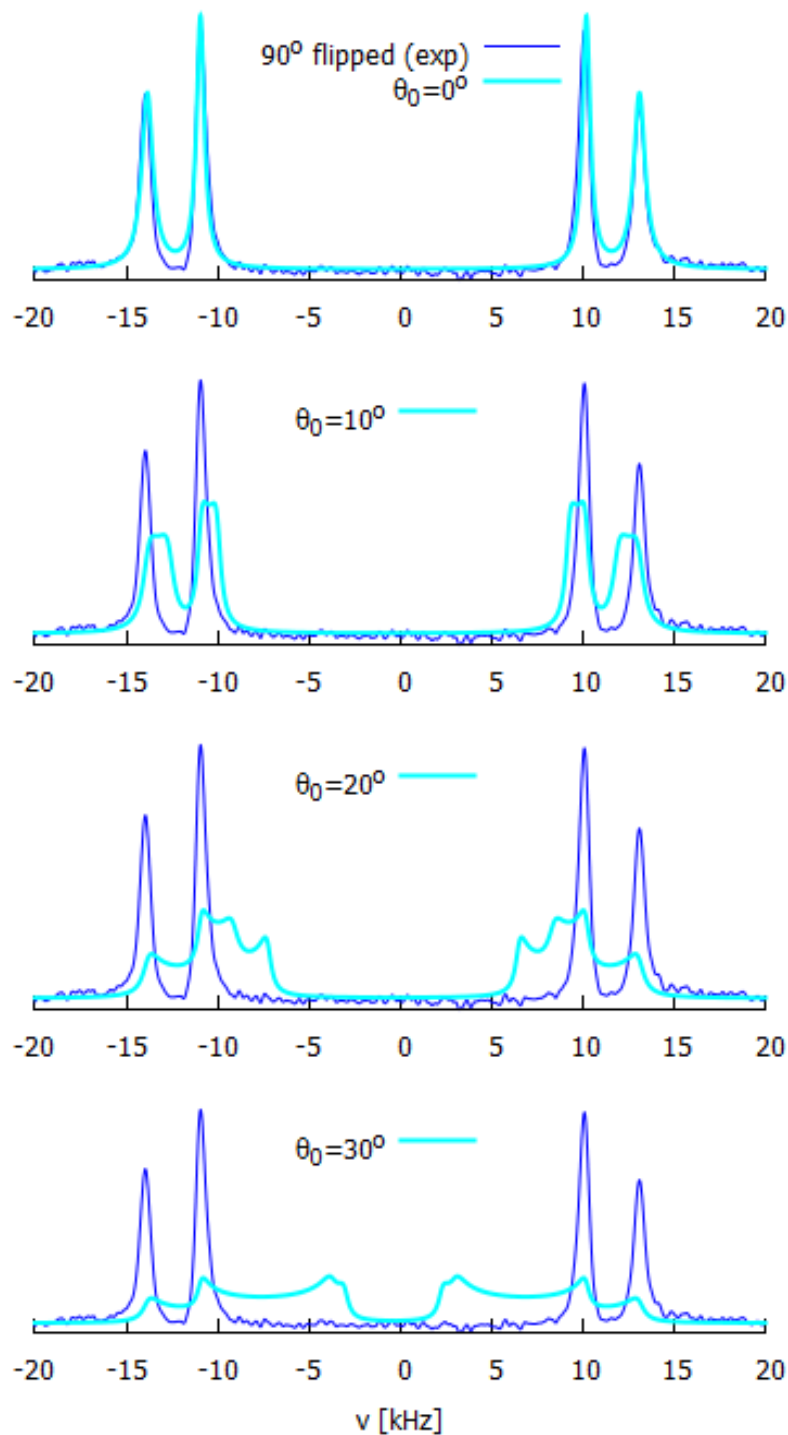


**Figure 3.** NMR spectrum of the 90o-flipped sample (blue) and the corresponding calculated spectra (cyan) for a single, uniformly distributed, director ( $\theta_0 = 0$ ) and for a hypothetical heliconical distribution of the director,  $\mathbf{n} = (\sin \theta_0 \cos kZ, \sin \theta_0 \sin kZ, \cos \theta_0)$ , with values of the “tilt” angle  $\theta_0 = 10^\circ, 20^\circ, 30^\circ$ .

It is clear from equations S.5 to 7 that the measured NMR spectrum can pick up variations of the angle of the director relative to the spectrometer magnetic field and that these variations are manifested as broadening of the spectral lines, in excess to their width at perfect alignment. The resolution of the experimental method sets a lower bound to the extent of variations that can be detected unambiguously on the measured spectra. With the simulation procedure described above we have found that, within the resolution of the experimental spectra, both the aligned sample spectrum and the  $90^\circ$ -flipped spectrum place an upper bound of  $5^\circ$  for possible variations of the angle of the director relative to the magnetic field. Accordingly, if it is assumed that, as a result of a hypothetical heliconical distribution, the director forms a constant angle  $\theta_0$  with the magnetic field, then it is directly deduced from the  $90^\circ$ -flipped spectrum that this angle should be below  $5^\circ$ . Of course variations of such a limited range could also be due to minor fluctuations of the director within the sample, not related to any heliconical distribution. In any case, the upper bound for  $\theta_0 < 5^\circ$ , set by the combined experimental and simulation resolution, is far below the values given for  $5^\circ$  in the literature<sup>2</sup> on the twist-bend nematic phase.

---

<sup>2</sup> (a) V. Borshch, Y.-K. Kim, J. Xiang, M. Gao, A. Jáklí, V. P. Panov, J. K. Vij, C. T. Imrie, M. G. Tamba, G. H. Mehl, and O. D. Lavrentovich, *Nat. Commun.* **4**, 2635 (2013).

(b) D. Chen, J. H. Porada, J. B. Hooper, A. Klitnick, Y. Shen, M. R. Tuchband, E. Korblova, D. Bedrov, D. M. Walba, M. A. Glaser, J. E. Maclennan, and N. A. Clark, *PNAS* **110**, 15931 (2013).

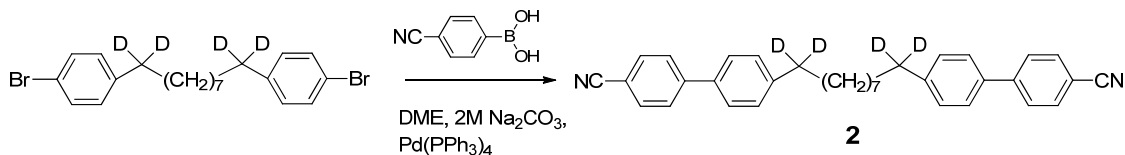
(c) L. Beguin, J. W. Emsley, M. Lelli, A. Lesage, G. R. Luckhurst, B. A. Timimi, and H. Zimmermann, *J. Phys. Chem. B* **116**, 7940 (2012).

(d) C. Meyer, G. R. Luckhurst, and I. Dozov, *Phys. Rev. Lett.* **111**, 067801 (2013).

(e) J. W. Emsley, M. Lelli, A. Lesage, and G. R. Luckhurst, *J. Phys. Chem. B* **117**, 6547 (2013).

(f) C. Greco, G. R. Luckhurst, and A. Ferrarini, *Phys. Chem. Chem. Phys.* **15**, 14961 (2013).

#### 4. Preparation of the target material



**Preparation of 1-d<sub>2</sub>, 9-d<sub>2</sub> -bis([1,1'-biphenyl]-4-carbonitrile) (2):** A solution of **1-d<sub>2</sub>, 9-d<sub>2</sub>-bis-(4-bromophenyl)nonane** (0.70g, 0.0015mol) and), (4-cyanophenyl)boronic acid (0.66g, 0.0045mol) and tetrakis(triphenylphosphine)palladium(0) (0.075g), were dissolved in degassed tetrahydrofuran under an inert atmosphere. After an hour a saturated aqueous solution of sodium carbonate (0.48g) was added drop wise and the reaction is refluxed overnight. The solvent was removed under reduced pressure and the organics separated by silica column chromatography using a mixture of dichloromethane and hexane 1:3 to afford the title compound as a white solid (0.51g, 67%).

<sup>1</sup>H NMR: δ<sub>H</sub> (400 MHz, CD<sub>2</sub>Cl<sub>2</sub>) 7.64 (4H, J = 8.5), 7.59 (4H, J = 8.5) 7.51 (4H, d, J 8.2), 7.29 (4H, d, J 8.16), 1.65-1.55 (4H, m), 1.40-1.20 (10H, m).

<sup>13</sup>C NMR: δ<sub>C</sub> (100 MHz, CDCl<sub>3</sub>) 145.6, 143.8, 132.6, 129.2, 127.5, 127.1, 119.2, 119.0, 110.5, 35.6, 31.4, 31.3, 29.4 (broad C-D), 29.3,

HPLC > 98.6%

### 5. DSC Trace of CB-C9-CB at 10°C min<sup>-1</sup>

